

**Electronic supplementary information for**

## **Electrospun Nanofibrous Adsorbent for Uranium Extraction from Seawater**

Siyuan XIE,<sup>‡a,b</sup> Xiyan LIU,<sup>‡a</sup> Bowu ZHANG,<sup>\*a</sup> Hongjuan MA,<sup>a</sup> Changjian LING,<sup>a</sup> Ming YU,<sup>a</sup>  
Linfan LI<sup>a</sup> and Jingye LI,<sup>\*a</sup>

<sup>a</sup> CAS Center for Excellence in TMSR Energy System, Shanghai Institute of Applied Physics, Chinese Academy of Sciences, No. 2019 Jialuo Rd., Jiading Dist., Shanghai, 201800, China. E-mail: [zhangbowu@foxmail.com](mailto:zhangbowu@foxmail.com); [jingyeli@sinap.ac.cn](mailto:jingyeli@sinap.ac.cn); Tel: +86-21-39194652; +86-21-39194505

<sup>b</sup> Graduate University of Chinese Academy of Sciences, No. 19A Yuquan Rd., Shijingshan Dist., Beijing, 100049, China

‡ Miss S. Y. XIE and Miss X. Y. Liu contributed equally to this work.

## Experiments and Characterizations

### S1 Chemicals and materials

Polyacrylonitrile (PAN) powder ( $M_w = 250,000$ ) was purchased from sigma-Aldrich Co., Ltd., USA. Polyvinylidene fluoride (PVDF) powder ( $M_w = 420,000$ ) was purchased from Solvay Chemicals Co., Belgium. An uranyl nitrate standard solution was purchased from Analytical Laboratory in Beijing Research Institute of Uranium Geology. N, N-dimethyl formamide (DMF), hydroxylamine ( $\text{NH}_2\text{OH}$ ) and sodium hydroxide (NaOH) and other chemicals were purchased from Sinopharm Chemical Reagent Co., Ltd., China. All chemicals were used without further purification. Deionized water was used for all experiments unless otherwise stated.

### S2 Preparation of polyamidoxime (PAO)

The PAO adsorbent was prepared by amidoximation of PAN powder (**Figure S6**). The details as follows, 32g hydroxylamine ( $\text{NH}_2\text{OH}$ ) was added and dissolved in a 500 ml round bottomed flask filled with 200 ml DMF. 17.5g sodium hydroxide (NaOH) was put into this solution and mixed with vigorous magnetic stirring for 15 minutes. Then, 20g PAN powder was added to the mixture above. After 6 hours reaction in  $75^\circ\text{C}$  water bath by continuous stirring, all of reactants were dissolved in solution and the resultants were placed in room temperature and rested overnight before further filtration. The filtrate of resultants was collected with paper-filter and stored in ampoule bottle for electrospinning. The concentration of PAO in filtrate is about  $0.1 \text{ g mL}^{-1}$ .

To determine the conversion of AN to AO group, the carbon content of resulted PAO were measured by elemental analysis (Table S1), and the conversion can be calculated according to equation 1.

$$C(\%) = \frac{3M_C M_{AO} - M_{AN} M_{AO} \omega_C}{3M_C (M_{AO} - M_{AN})} \times 100\% \quad (1)$$

Where  $\omega_C$  is carbon weight content of obtained PAO listed in Table S1,  $M_C$ ,  $M_{AO}$  and  $M_{AN}$  are the formula mass of carbon, AO and AN, respectively. Accordingly, the conversion of PAN here is calculated as 76.8%. The chemical structure was characterized by FT-IR and XPS spectroscopy as shown in **Figure S7**.

### S3 Porosity measurement of PAO/PVDF composite mats

Generally, porosity of materials is related to the inherent density and apparent density of materials. To determine the inherent density of PAO and PVDF, the solution of PAO and PVDF were casted on freshly cleaned glass flats, respectively and dried naturally at room temperature. After the solvent volatilizing completely, PAO and PVDF films were obtained by peeling off from glass flats. Herein, we make some hypothesis for simplification. For instance, the film by casting is assumed as nonporous and dense, and the thickness of casting film and electrospun mats are also supposed to be uniform completely. Therefore, we determined the volume by measuring the surface area and thickness of the film and mats. Wherein, the thickness was measured by a micrometer (**Table S2**). The weight were measured by weighting. And the inherent density of PAO and PVDF, the apparent density of nanofibrous composite mats can be calculated by equation 2.

$$\rho = \frac{W}{V} = \frac{W}{SH} \quad (2)$$

Where  $\rho$  is the density of samples;  $W$  and  $V$  are the weight and volume of samples;  $S$  and  $H$  are the surface area and thickness of samples, respectively. Herein, the mats has two components, and its inherent density obviously depends on the inherent density of PAO and PVDF, and weight content of PAO in mats is the coefficient. Therefore, the inherent density of mat can be calculated as follows:

$$\rho_{Mi} = \rho_O x + \rho_F (1 - x) \quad (3)$$

Wherein,  $\rho_{Mi}$ ,  $\rho_O$  and  $\rho_F$  are the inherent density of mat, PAO film and PVDF film.  $x$  is the weight content of PAO in PAO/PVDF mats. Thus, the porosity of PAO/PVDF composite mats can be calculated according to equation 4.

$$p(\%) = \frac{\rho_{Ma}}{\rho_{Mi}} \times 100\% = \frac{\rho_O \rho_F - \rho_O \rho_{Ma} - x \rho_{Ma} (\rho_F - \rho_O)}{\rho_O \rho_F} \times 100\% \quad (4)$$

Where  $p$  is the porosity of mats;  $\rho_O$  and  $\rho_F$  are the inherent density of PAO and PVDF, respectively;  $\rho_{Ma}$  is apparent density of PAO/PVDF mats.  $x$  is the weight content of PAO in

PAO/PVDF composite mats.

#### **S4 Preparation of simulated seawater**

350 g baysalt (obtained from salt fields in Qingdao city of Shandong province, without any refining) and 0.42 g anhydrous sodium carbonate solid were dissolved in 10 L deionized water. Then baysalt solution was stand for 48 hours and filtrated with filter cloth to remove the sands and other impurities. The common co-existing ions such as U, V, Fe, Co, Ni, Cu, Zn and Pb in this clear baysalt solution were determined by a method of concentrated extraction with a CHELEX-100 resin and ICP-MS (Inductively Coupled Plasma-Mass Spectrum, Nex ION 300 Perkin Elmer). In order to create a simulated seawater system with 100 times of concentrations in real seawater, 3300  $\mu\text{l}$  uranyl nitrate standard solution, 1500  $\mu\text{l}$  ammonium metavanadate standard solution, 1000  $\mu\text{l}$  Fe (NO<sub>3</sub>)<sub>3</sub> standard solution, 50  $\mu\text{l}$  Co (NO<sub>3</sub>)<sub>2</sub> standard solution, 1000  $\mu\text{l}$  Ni (NO<sub>3</sub>)<sub>2</sub> standard solution, 600  $\mu\text{l}$  Cu (NO<sub>3</sub>)<sub>2</sub> standard solution, 4000  $\mu\text{l}$  Zn (NO<sub>3</sub>)<sub>2</sub> standard solution and 30  $\mu\text{l}$  Pb (NO<sub>3</sub>)<sub>2</sub> standard solution were added to the solution. All standard solutions with 1000 ppm concentration were offered by SPEX CertiPrep Company. The exact concentration of U, V, Fe, Co, Ni, Cu, Zn and Pb were determined by ICP-MS after concentrating with CHELEX-100 resin. The Mg and Ca were directly measured by ICP-AES (Inductively Coupled Plasma-Atomic Emission Spectrometer, Optima 8000 Perkin Elmer). The pH value of the solution was adjusted to 8.0 before adsorption test by the sodium carbonate solution (2 mol L<sup>-1</sup>) and nitric acid solution (2 mol L<sup>-1</sup>).

#### **S5 General Characterization**

FT-IR spectra of PAN and PAO were collected by scanning the potassium bromide tablets of samples on transmission module. While the spectra of mats with different PAO content were obtained by scanning the nanofibrous mats on attenuated total reflection (ATR) module. All the FT-IR spectra were performed on a Bruker Optics TENSOR 27 FT-IR Spectrometer and were averaged over 32 scans at 4 cm<sup>-1</sup> resolution obtained in the range of 600~4000 cm<sup>-1</sup>. The microscopic morphology of nanofibrous mats were observed with a JSM-6700F scanning electron microscope (JEOL, Japan). Samples were sputtered with 10 nm gold layer to enhance the electrical conductivity. Elemental analysis was carried out with an Elementar Vario EL III

Elemental Analyzer. All samples were dried in a vacuum oven at 60°C for 24 h before testing. The pore size distribution was measured by using Mercury Porosimetry (autoporeIV9500, Micrometrics Instrument Co., USA) and Surface Area and Pore Size Analyzer (V-Sorb 2800TP, Gold APP Instruments Co., China). The intrusion pressure range of mercury was within 0.1-60000 psi. The samples were degassed overnight in vacuum at 180 °C for 6 hours and N<sub>2</sub> gas was used to BET surface area. The relative pressure range of  $p/p_0$  from 0.05 to 0.2 was used for calculating the BET surface area. The water static contact angle of nanofibrous mats was measured on a KSV ATTENSION Theta Optical Tensionmeter. A 5  $\mu$ L water drop from needle tip was stroked onto the sample surface. Shape of the droplet was recorded by a digital camera and static contact angle was calculated according to images taken by evaluation software provided from the instrument manufacturer. The mechanical property tests were obtained from a QJ210 electronic tensile testing machine (Shanghai Tilting Technology Science and Technology Instrument Co., Ltd.) at room temperature. The samples were stretched at a speed of 2 mm/min. All of samples are cut into 10 mm width and 20 mm length. The final mechanical properties were evaluated from 5 parallel measurements.

## Tables and Figures

**Table S1.** The controlling of PAO content in electrospun nanofibrous mats by adjusting injection rate of PAO, PVDF solution

		PAO mats	PAO/PVDF mats			PVDF mats
Injection rate (mL/h)	PVDF	0	0.2	0.4	0.8	0.4+0.4
	PAO	0.4+0.4	0.4	0.4	0.4	0
Theoretical PAO content		100	66.7	50	33.3	0
Actual PAO content		100	70.8	56.6	18.4	0

**Table S2.** The porosity tests of electrospun nanofibrous mats

		Inherent density (mg/mm <sup>3</sup> )	Apparent density (mg/mm <sup>3</sup> )	Porosity (%)	Thickness (μm)
PAO film		1.21	---	---	140
PVDF film		3.52	---	---	150
PAO mat		---	0.573	52.6	80
PAO/PVDF composite film	70.8%	---	0.509	66.0	80
	56.6%	---	0.525	69.0	118
	18.4%	---	0.366	85.9	70
PVDF mat		---	0.509	85.5	54

**Table S3.** Ions concentration of actual and simulated sea water

Element	U	V	Fe	Co	Ni	Cu	Zn	Pb	Mg	Ca
<b>Actual</b>										
Seawater (ppb) <sup>1,2,3</sup>	3.3	1.5-2.5	1.0- 2.0	0.05	1.0	0.6	4.0	0.03	1.3x1 0 <sup>6</sup>	0.4 x10 <sup>6</sup>
<b>Simulated</b>										
Seawater (ppb)	330	152	141	5.3	101	65	408	34.6	1.2x1 0 <sup>5</sup>	0.6 x10 <sup>5</sup>
Ions <sup>1,3-5</sup>	UO <sub>2</sub> (CO <sub>3</sub> ) <sub>3</sub> <sup>4-</sup> UO <sub>2</sub> (CO <sub>3</sub> ) <sub>2</sub> <sup>2-</sup>	VO <sub>2</sub> (OH) <sub>3</sub> <sup>2-</sup> VO <sub>3</sub> <sup>-</sup> HVO <sub>4</sub> <sup>2-</sup>	Fe <sup>3+</sup>	Co <sup>2+</sup>	Ni <sup>2+</sup>	Cu <sup>2+</sup>	Zn <sup>2+</sup>	Pb <sup>2+</sup>	Mg <sup>2+</sup>	Ca <sup>2+</sup>



**Table S4.** Elemental analysis of PAO powder

	<b>N (%)</b>	<b>C (%)</b>	<b>H (%)</b>
<b>1</b>	30.92	45.37	6.77
<b>2</b>	31.12	45.48	6.76
<b>3</b>	30.9	45.19	6.81
<b>Average</b>	30.98	<b>45.35</b>	6.78

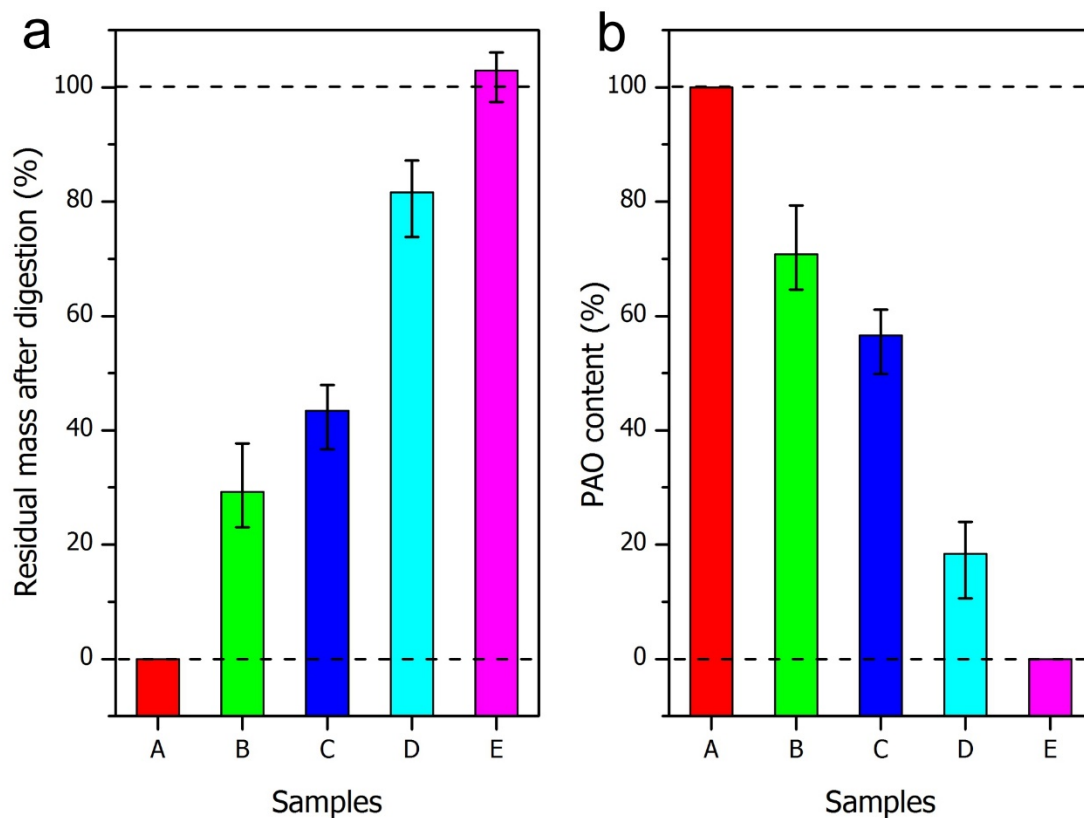


**Figure S1.** (a) The residual mass of electrospun nanofibrous mats with different content of PAO; (b) the calculated PAO content of various electrospun mats. (A: PAO mat; B, C, D: PAO/PVDF mats; E: PVDF mat)

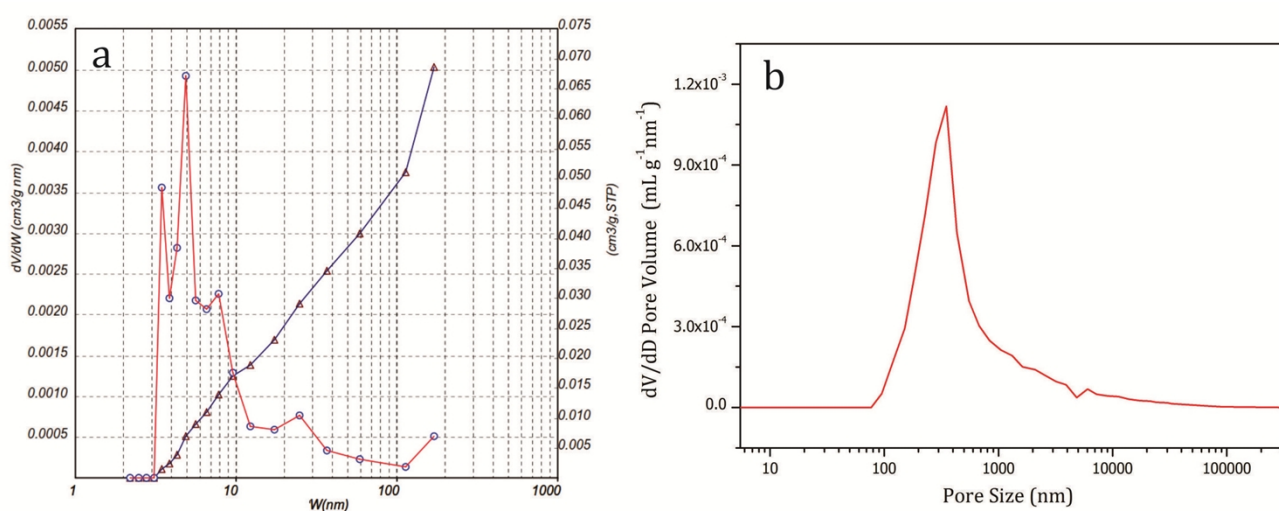


**Figure S2.** the pore size distribution of PAO mat determination by: (a) BET nitrogen absorption and (b) Mercury porosimetry.



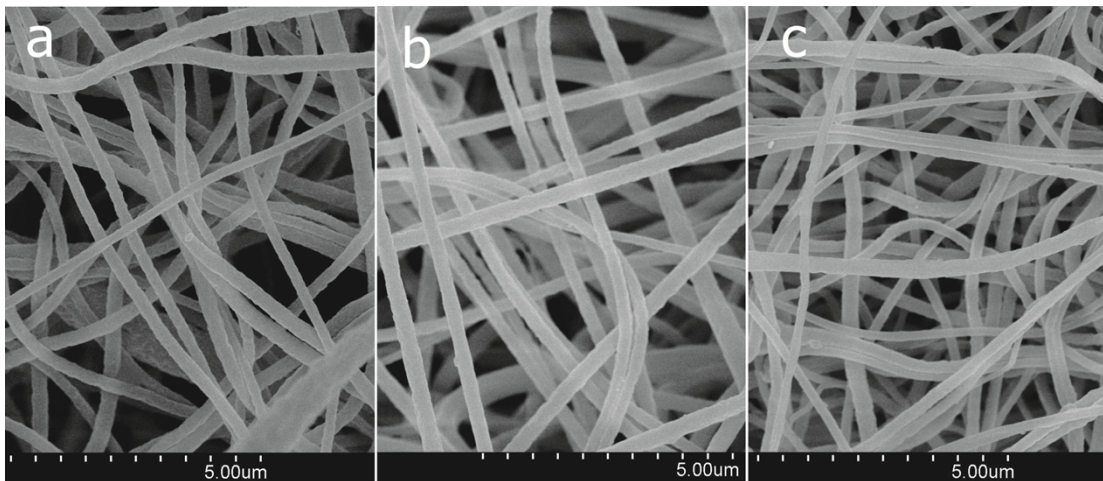
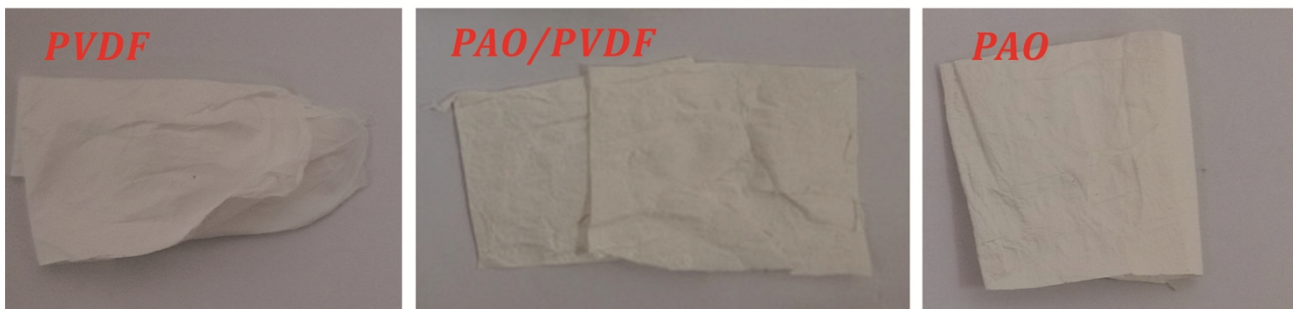


**Figure S3.** the SEM images of PAO/PVDF composite mats with different PAO content: (a) 70.8%, (b) 18.4% and (c) 0%.

### *Before Adsorption*



### *After Adsorption*

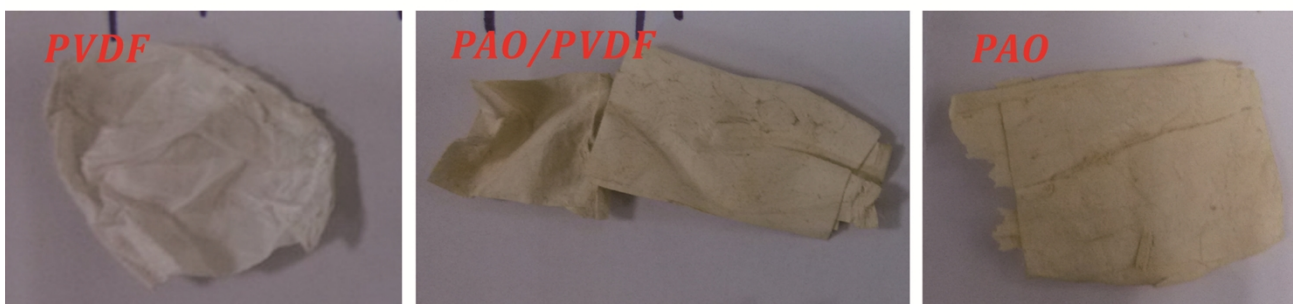


**Figure S4.** The pictures of different electrospun nanofibrous mats before and after adsorption: pure PVDF mats, PAO/PVDF composites mats with 70.8% of PAO and pure PAO mats.

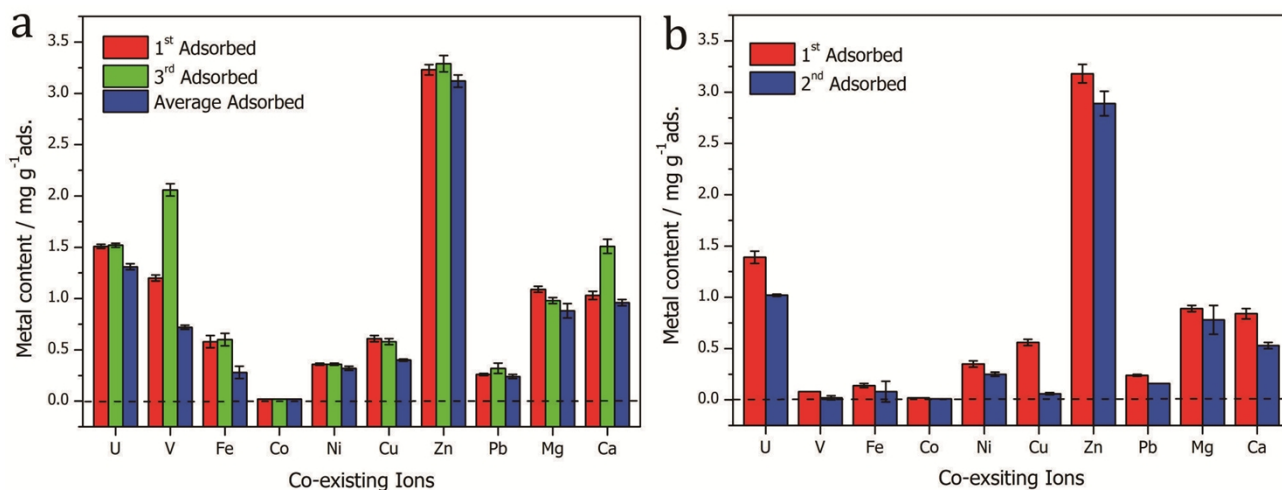


**Figure S5.** Multiple entry of nanofibrous PAO/PVDF composite mat with 70.8% PAO content. (a) Metal content by mat adsorption: 1<sup>st</sup> adsorbed means the metal content in mats after 1<sup>st</sup> adsorption; 3<sup>rd</sup> adsorbed represents the metal content in mat after 3<sup>rd</sup> adsorption, which had gone through twice adsorption/desorption cycle; Average adsorbed is the average of 1<sup>st</sup> desorbed, 2<sup>nd</sup> desorbed and 3<sup>rd</sup> adsorbed, which indicates the average capacity of mat in every cycle. (b) Metal content in desorption solution: 1<sup>st</sup> desorbed depicts the metal content in desorbed solution from 1<sup>st</sup> desorption; 2<sup>nd</sup> desorbed is that from 2<sup>nd</sup> desorption of the mat has gone through 2<sup>nd</sup> adsorption.

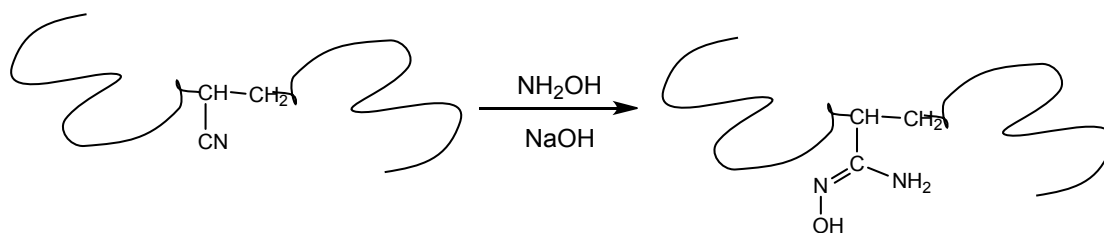


**Figure S6.** The scheme of amidoximation of PAN powder

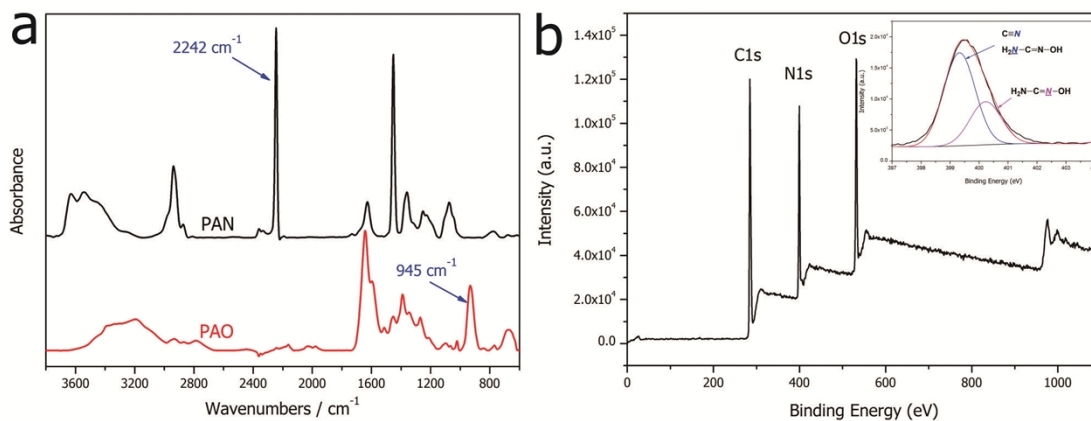


**Figure S7.** (a) FT-IR spectra PAN and PAO powder and (b) XPS wide scan spectrum of PAO. The insert in (b) is high resolution N1s spectrum of PAO.



**Figure S8.** The photograph of electrospinning equipment (TL01, Shenzhen TONGLI Micro & Nano Tech. LTD.)

## References

1. H. Sodaye et al. Extraction of uranium from the concentrated brine rejected by integrated nuclear desalination plants. *Desalination* 235 (2009) 9–32.
2. Riley J.P, Skirrow G. *Chemical oceanography* [M]. 2nd Ed, 1975: 417.

3. Wang D, Sañudo-Wilhelmy S.A., Development of an analytical protocol for the determination of V (IV) and V (V) in seawater: Application to coastal environments. *Marine Chemistry* 112 (2008) 72–80.
4. Ladd, K. V. 1974. The distribution and assimilation of vanadium with respect to the tunicate *Ciona intestinalis*. Ph.D. thesis, Brandeis Univ. p. 108
5. K.K. Turekian, *Handbook of Geochemistry*, K.H. Wedepohl, Springer-Verlag, Berlin 1969 p. 309